

Polymer solar cells fabricated with 4,8-bis(2-ethylhexyloxy)benzo[1,2-*b*:4,5-*b'*]dithiophene and alkyl-substituted thiophene-3-carboxylate-containing conjugated polymers: Effect of alkyl side-chain in thiophene-3-carboxylate monomer on the device performance

Min Ju Cho^a, Jangwon Seo^a, Kai Luo^a, Kyung Hwan Kim^b, Dong Hoon Choi^{b,**}, Paras N. Prasad^{a,*}

^a Department of Chemistry, University at Buffalo, State University of New York, Buffalo, NY 14260, USA

^b Department of Chemistry, Research Institute for Natural Sciences, Korea University, Seoul 136-701, Republic of Korea

ARTICLE INFO

Article history:

Received 31 May 2012

Received in revised form

26 June 2012

Accepted 5 July 2012

Available online 16 July 2012

Keywords:

Bulk heterojunction

Copolymerization

PCBM

ABSTRACT

Four alkyl-substituted thiophene-3-carboxylate containing donor–acceptor (D–A) copolymers were designed, synthesized, and characterized. Thiophene-3-carboxylate was used as a weak electron acceptor unit in the copolymers to provide a deeper highest occupied molecular orbital (HOMO) level for obtaining a higher open-circuit voltage in polymer solar cells (PSCs). The resulting bulk heterojunction PSCs, made of the copolymers and [6,6]-phenyl-C71-butyric acid methyl ester (PC₇₁BM), exhibited different short circuit currents (J_{SC}) and open-circuit voltages (V_{OC}), depending on the length of alkyl side-chain in the thiophene-3-carboxylate unit. Among all fabricated photovoltaic (PV) devices, PC2:PC₇₁BM (1:1 wt. ratio) showed the highest efficiency with the highest J_{SC} of 10.5 mA/cm². Although PC5:PC₇₁BM (1:1) displayed the highest V_{OC} of 0.93 V, the device efficiency was observed to be poor, which is due to poor nanophase segregation. This comparison shows that the side-chain of thiophene carboxylate in these copolymers plays a very important role in the device efficiency.

© 2012 Elsevier Ltd. All rights reserved.

1. Introduction

Polymer solar cells (PSCs) are of interest because of their potential to be fabricated by low cost of device fabrication using solution-processing technology such as spin-coating, drop-casting, and ink-jet printing, etc. They also offer potential possibility for future flexible photovoltaic (PV) devices [1–5]. To achieve a high power conversion efficiency (PCE), highly crystalline polymer donors and organic soluble fullerene acceptors have often been employed for solution-processed bulk heterojunction (BHJ) PSCs, which have been shown to have a PCE approaching 5.0–8.5% [6–10]. PCE is the product of the short-circuit current density (J_{SC}), the open circuit voltage (V_{OC}), and the fill factor (FF) divided by the incident light intensity. Therefore, for achieving improved J_{SC} , it is necessary that the polymeric donors should have a broad absorption from the visible to near-infrared (NIR) wavelength range of the solar spectrum [11–13], because the light absorbing

capability is directly related to the value of J_{SC} . Recently, efficient low-bandgap copolymers with broad absorption spectra were developed by using electron donating units, such as cyclopenta[2,1-*b*:3,4-*b'*]dithiophene [14,15], dithieno[3,2-*b*:2',3'-*d*]silole [16], and benzo-[1,2-*b*:4,5-*b*]dithiophene [10,13], and electron withdrawing units, such as 2,1,3-benzothiadiazole [17], diketopyrrolo[3,4-*c*]pyrrole-1,4-dione [18], thieno[3,4-*b*]thiophene [10,13], and thieno[3,4-*c*]pyrrole-4,6-dione [19]. V_{OC} is also one of the important factors to obtain a high PCE value. V_{OC} of PSC is commonly proportional to the difference between the HOMO of the electron donating polymeric unit and the LUMO of the electron accepting PCBM within the active layer [20]. Therefore, it is desirable for efficient PSCs to design an electron donor polymer with a lower HOMO level. Some kinds of donor–acceptor (D–A) copolymers have been successfully used for achieving high V_{OC} s in PSCs by choosing fluorene, silafluorene, and carbazole derivatives as electron donating groups. These derivatives consist of well-known wide-band-gap semiconducting materials. However, most of these polymers have suffered from a low J_{SC} in PSCs, except for some specific polymers [8,9]. Among these copolymers, only a few polymers, containing a thieno[3,4-*c*]pyrrole-4,6-dione (TPD) acceptor unit, showed relatively higher V_{OC} and J_{SC} compared to the conventional P3HT:PCBM BHJ PSC [21–24]. Although the TPD-

* Corresponding author. Tel.: +1 716 645 6800; fax: +1 716 645 6945.

** Corresponding author.

E-mail addresses: dhchoi8803@korea.ac.kr (D.H. Choi), pnprasad@buffalo.edu (P.N. Prasad).

based polymers with PCBM exhibited a high efficiency in PSC, the synthesis of TPD is quite complicated to produce a desirable amount of corresponding polymers. It is quite intriguing that the alkyl-substituted thiophene-3-carboxylate (TC) groups act as electron-withdrawing units in the main-chain of conjugated copolymers. The TC unit with different alkyl groups can be easily prepared through a simple synthetic procedure. In the past, several research groups reported that PSCs with TC-based polymers and PCBM exhibited a much better PV performance, with moderate high PCE and V_{OC} values than P3HT:PCBM-based PSCs. For example, Hu *et al.* reported a new regiorandom PCTBDT which is an alternating copolymer containing benzodithiophene (BDT) and hexyl thiophene-3-carboxylate [25]. The PSC obtained from PCTBDT:PCBM blends exhibited PCE value up to 2.32%, with V_{OC} of 0.80 V. Zhao's group demonstrated **PL5** copolymer consisting of BDT and butyl thiophene-3-carboxylate. The PCE and V_{OC} values of the PV devices based-on **PL5** were measured to be 2.06% and 0.75 V, respectively [26]. In our previous study, we also synthesized the TC-based copolymer (PBDT-3MT) containing BDT and methyl thiophene-3-carboxylate for fabricating PSCs. The PV device composed of PBDT-3MT:PCBM blends exhibited a high PCE value of 4.52%, with $V_{OC} = 0.86$ V [27]. Herein, we have synthesized a series of copolymer bearing 4,8-bis(2-ethylhexyloxy)benzo[1,2-*b*:4,5-*b'*]dithiophene and the TC unit, and investigated the effect of alkyl side chain (e.g. methyl, butyl, octyl, and 2-ethylhexyl groups) in the TC unit on the PV device performances. Also, we systematically studied the effect of alkyl side-chain in TC unit of these copolymers on the optical properties, film morphology, carrier mobility in organic thin film transistor (OTFT), as well as on the photovoltaic performance. These results provide useful information on how to control the V_{OC} and PCE value of OPV devices, based-on the structural variation in copolymers containing TC unit.

2. Experimental section

2.1. Materials

All reagents were purchased from the Sigma–Aldrich Co. and used without further purification, unless stated otherwise. Reagent grade solvents used in this study were freshly dried under standard distillation methods. The 2,5-dibromothiophene-3-carboxylic acid (**1**), **2b**, **3**, and PC2 (PBDT-3MT) were prepared according to published procedures [27,28].

2.2. Instrumental analysis

^1H NMR spectra were recorded on a Varian NMR 400 and 500 MHz spectrometer using deuterated chloroform purchased from Cambridge Isotope Laboratories, Inc. The molecular weight of the polymers was determined on a Waters 1525/2414 gel permeation chromatography (GPC) with polystyrene as a standard. Thermal gravimetric analysis (TGA) was conducted on a Mettler TGA50 thermal analysis system at a heating rate of $10\text{ }^\circ\text{C}/\text{min}$. The absorption spectra of the film samples and of chloroform solutions were obtained using a Shimadzu UV-3101 PC spectrophotometer in the wavelength range of 300–800 nm. The redox property of the synthesized copolymers was examined by cyclic voltammetry (Model: EA161 eDAQ). The electrolyte solution employed was 0.10 M tetrabutylammonium hexafluorophosphate (Bu_4NPF_6) in freshly dried acetonitrile. The Ag/AgCl and Pt wire (0.5 mm in diameter) electrodes were utilized as the reference and the counter electrodes, respectively. The scan rate was at 50 mV/s. Atomic force microscopy (AFM, Advanced Scanning Probe Microscope, XE-100, PSIA), operating in the tapping mode with a silicon cantilever, was used to characterize the surface morphologies of the samples.

The film samples were fabricated by spin-coating on silicon wafer, followed by drying at $90\text{ }^\circ\text{C}$ for 10 min.

2.3. Organic thin film transistor (OTFT) device fabrication and characterization

For the characterization of TFT performance, a bottom gate top contact device geometry was employed. On a heavily n-doped Si/SiO₂ substrate, spin-coated films of copolymers were prepared from chloroform as the solvent. Surface modification was carried out with octyltrichlorosilane (OTS) to make the dielectric surface hydrophobic. The source and the drain electrodes were then thermally evaporated (100 nm) through a shadow mask, with channel width and length of 1500 μm , and 100 μm , respectively. All the field effect mobilities were extracted in the saturation regime using the relationship $\mu_{\text{sat}} = (2I_{\text{DS}}L)/(WC(V_{\text{G}} - V_{\text{th}})^2)$, where I_{DS} means saturation drain current, C is capacitance of SiO₂ dielectric, V_{G} is gate bias, and V_{th} is threshold voltage. The device performance was evaluated in air using a 4200-SCS semiconductor characterization system.

2.4. Photovoltaic device fabrication and characterization

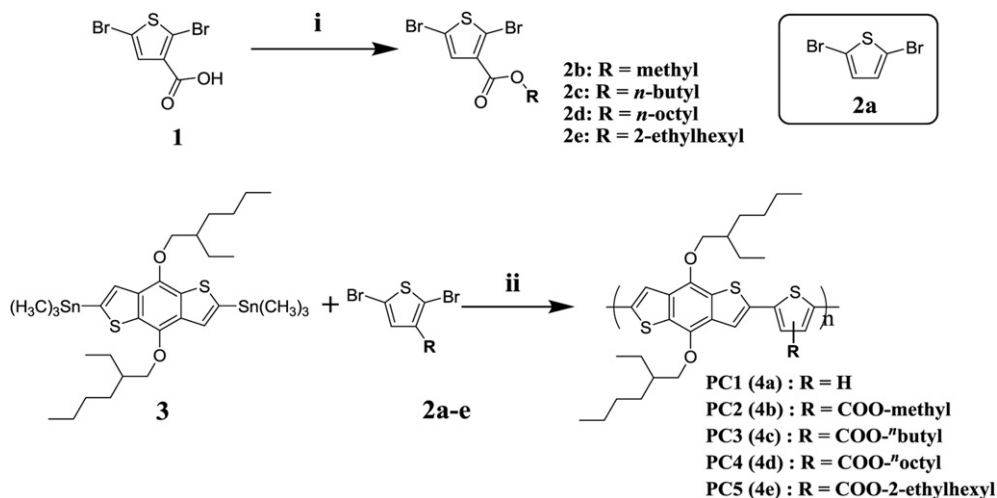
All devices reported here were fabricated on indium tin oxide (ITO) coated glass substrates. A 30 nm layer of PEDOT:PSS was spin coated on the top of ITO and baked at $120\text{ }^\circ\text{C}$ for 10 min. Subsequent device processing was performed in a glove box under nitrogen atmosphere. A polymer:PC₇₁BM blend film was spin coated on top of the PEDOT:PSS layer using a *o*-dichlorobenzene (*o*-DCB) solution and was dried at $90\text{ }^\circ\text{C}$ for 10 min. Finally, a ~ 100 nm thick lithium fluoride (LiF)/aluminum (Al) electrode was deposited by a thermal evaporator (vacuum at 10^{-6} – 10^{-7} Torr) to produce a 0.0425 cm^2 active area using a mask. The *I*–*V* characteristics were measured by a computerized Keithley 2400 source meter in the dark and under AM 1.5G illumination at $100\text{ mW}/\text{cm}^2$ supplied by a solar simulator (Oriel, 1000 W). The spectral response was measured using a tungsten–halogen light source combined with a monochromator (Spectra Pro 2300, Acton Research). The light was filtered through the monochromator for the UV, visible and IR wavelength range to remove harmonics and was modulated using an optical chopper at 350 Hz. The resulting photocurrent in the photovoltaic cell was measured using a lock-in amplifier (SR-830, Stanford Research). The power of the monochromatic light was measured by using a calibrated optical power meter and a photodetector (Coherent Fieldmax II with UV to IR sensor heads and a Thorlabs PM100). All equipment and data acquisition were controlled by LabView.

2.5. Synthesis of alkyl 2,5-dibromothiophene-3-carboxylates: general procedure

2,5-Dibromothiophene-3-carboxylic acid (**1**) (1.0 mmol) and K_2CO_3 (3.0 mmol) were dissolved in 20 mL of dried dimethylformamide (DMF), and alkyl bromide/iodide (2.0 mmol) was added in portions. The mixture was warmed and stirred at $80\text{ }^\circ\text{C}$ for 10 h. After the reaction was complete, the mixture was poured into 200 mL of water bearing 5 mL of 1 M HCl. The solution was washed with ether, and dried with Na_2SO_4 . The ether was removed with a rotary evaporator and the products (**2b**–**e**) were purified by silica-gel column chromatography.

2.5.1. Butyl-2,5-dibromothiophene-3-carboxylate (**2c**)

2c was synthesized with 2,5-dibromothiophene-3-carboxylic acid (**1**) and 1-bromobutane by following the general procedure. The final product, colorless oil, was obtained with a 92% yield. ^1H



Scheme 1. Synthetic procedure for monomers and polymers: i) alkyl bromide or alkyl iodide, K_2CO_3 , DMF, 80 °C, 10 h, ii) $\text{Pd}(\text{PPh}_3)_4$, toluene/DMF (9:1, v/v), 110 °C, 60 h.

NMR (400 MHz, CDCl_3 , δ , ppm): 7.38 (s, 1H), 4.29 (t, 2H), 1.78–1.58 (m, 2H), 1.52–1.41 (m, 2H), 0.91 (t, 3H).

2.5.2. Octyl-2,5-dibromothiophene-3-carboxylate (**2d**)

2d was synthesized with 2,5-dibromothiophene-3-carboxylic acid (**1**) and 1-bromooctane by following the general procedure. The final product, a white powder, was obtained with an 88% yield. ^1H NMR (400 MHz, CDCl_3 , δ , ppm): 7.40 (s, 1H), 4.31 (t, 2H), 1.79–1.56 (m, 2H), 1.35–1.18 (m, 10H), 0.90 (t, 3H).

2.5.3. 2-Ethylhexyl-2,5-dibromothiophene-3-carboxylate (**2e**)

2e was synthesized with 2,5-dibromothiophene-3-carboxylic acid (**1**) and 2-ethylhexyl-1-bromide by following the general procedure. The final product, colorless oil, was obtained with an 82% yield. ^1H NMR (400 MHz, CDCl_3 , δ , ppm): 7.44 (s, 1H), 4.32 (t, 2H), 2.11–1.89 (m, 1H), 1.31–1.21 (m, 8H), 0.89–0.82 (m, 6H).

2.6. Synthesis of copolymers: general procedure

To a 10 mL three-necked flask, bis(trimethylstannyl)-monomer (0.2 mmol), dibromo-monomer (0.2 mmol), and $\text{Pd}(\text{PPh}_3)_4$ (0.012 g, 0.01 mmol) were dissolved in anhydrous toluene (18 mL) and dimethylformamide (DMF) (2 mL). The reaction mixture was heated to 110 °C and stirred for 60 h. The crude product was collected by precipitating in methanol (200 mL), and subjected to Soxhlet extractions with acetone and CHCl_3 in succession. The pure polymer was collected from the CHCl_3 extracted after removal of the solvent.

2.6.1. Synthesis of PC1 (**4a**)

4a was synthesized with 4,8-bis(2-ethylhexyloxy)benzo[1,2-*b*:4,5-*b'*]dithiophene (**3**) and 2,5-dibromothiophene (**2a**) by following the general procedure. The final product, a red powder, was obtained with a 64% yield. ^1H NMR (400 MHz, CDCl_3 , δ , ppm):

7.20–6.75 (br, 4H), 4.20–3.82 (br, 4H), 1.85–1.42 (br, 18H), 1.30–0.89 (br, 12H). GPC: $M_w = 8.2$ kDa, $M_n = 4.3$ kDa, PDI = 1.9. TGA: $T_d = 326$ °C.

2.6.2. Synthesis of PC3 (**4c**)

4c was synthesized with monomer **3** and butyl-2,5-dibromothiophene-3-carboxylate (**2c**) by following the general procedure. The final product, a red powder, was obtained with a 75% yield. ^1H NMR (500 MHz, CDCl_3 , δ , ppm): 7.95 (br, 1H), 7.73–7.35 (br, 2H), 4.38–4.08 (br, 6H), 1.89–1.25 (br, 22H), 0.90–1.21 (br, 15H). GPC: $M_w = 40.9$ kDa, $M_n = 15.3$ kDa, PDI = 2.7. TGA: $T_d = 318$ °C.

2.6.3. Synthesis of PC4 (**4d**)

4d was synthesized with monomer **3** and octyl-2,5-dibromothiophene-3-carboxylate (**2d**) by following the general procedure. The final product, a red powder, was obtained with a 71% yield. ^1H NMR (500 MHz, CDCl_3 , δ , ppm): 7.93 (br, 1H), 7.71–7.57 (br, 2H), 4.32–4.21 (br, 6H), 1.91–1.42 (br, 22H), 1.30–0.82 (br, 23H). GPC: $M_w = 81.0$ kDa, $M_n = 28.7$ kDa, PDI = 2.8. TGA: $T_d = 327$ °C.

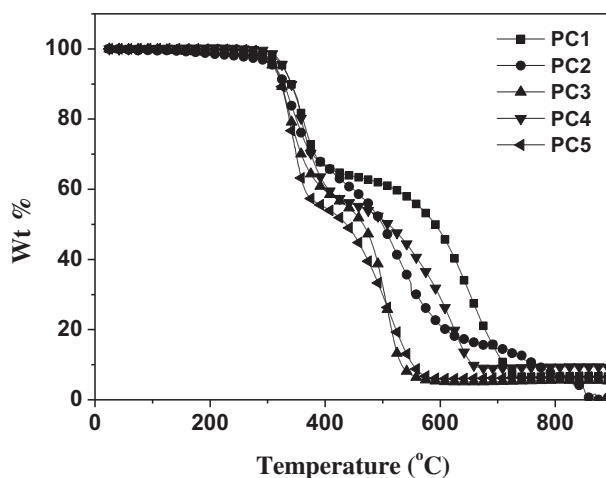


Fig. 1. Thermogravimetric analysis (TGA) plot of the copolymers with a heating rate of 10 °C/min in an atmosphere of N_2 .

Table 1
Physical properties of copolymers.

Polymer	Yield [%]	M_n [kDa]	M_w [kDa]	PDI	T_d [°C]
PC1	64	4.3	8.2	1.9	326
PC2	77	26.9	92.0	3.4	320
PC3	75	15.3	40.9	2.7	318
PC4	71	28.7	81.0	2.8	327
PC5	66	142.4	209.7	1.5	317

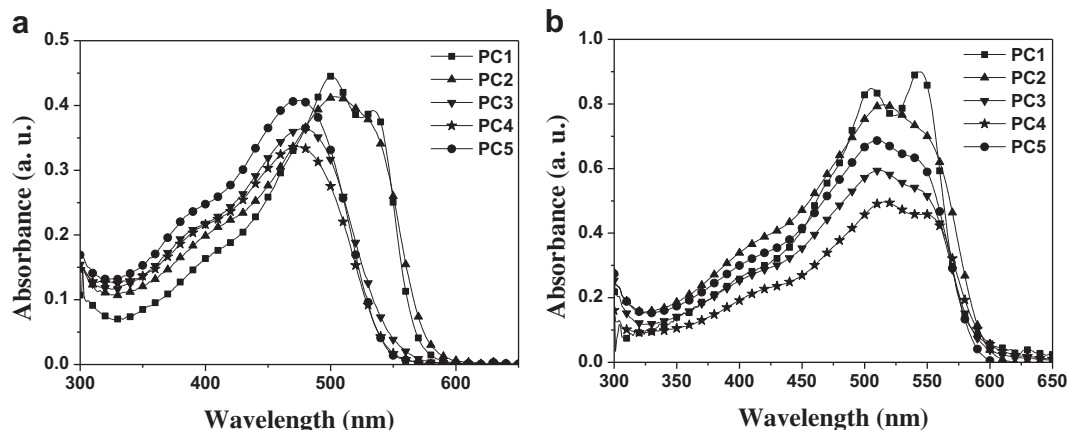


Fig. 2. UV-vis absorption spectra of copolymers in the *o*-DCB solution (a) and in the film state (b).

2.6.4. Synthesis of PC5 (4e)

4e was synthesized with monomer **3** and 2-ethylhexyl-2,5-dibromothiophene-3-carboxylate (**2e**) by following the general procedure. The final product, a red powder, was obtained with a 66% yield. ^1H NMR (500 MHz, CDCl_3 , δ , ppm): 7.94 (br, 1H), 7.75–7.53 (br, 2H), 4.35–4.12 (br, 6H), 1.89–1.18 (br, 27H), 1.15–0.81 (br, 18H). GPC: $M_w = 209.7$ kDa, $M_n = 142.6$ kDa, PDI = 1.5, TGA: $T_d = 317$ °C.

3. Results and discussion

3.1. Synthesis and characterization

The general synthetic procedure for the monomers and the copolymers is outlined in Scheme 1. Monomers, **2b–e** were easily synthesized by using 2,5-dibromothiophene-3-carboxylic acid (**1**) and alkyl bromide/iodide in the K_2CO_3 base. In order to investigate the effect of alkyl side-chain in TC unit of copolymers on PV device performance, we selected the methyl, butyl, octyl, and 2-ethylhexyl groups as side-chain moieties in the TC unit. Polymers, PC2–5 were synthesized by using the Stille coupling reaction of monomer **3** with monomers **2b–e** in a mixture of toluene/DMF *co*-solvent in the presence of $\text{Pd}(\text{PPh}_3)_4$ as a catalyst. In particular, PC1 containing only thiophene unit was also synthesized with the same method as a control sample, to compare the effect of the carboxylate substituents of PC2–5 on the PSC performances. All copolymers showed good solubility in common organic solvents such as chloroform, THF, toluene, and *o*-dichlorobenzene (*o*-DCB). The molecular weights and the polydispersity indices (PDIs) of copolymers were measured by gel permeation chromatography (GPC) with

tetrahydrofuran (THF) as eluent and polystyrene as the standard are listed in Table 1.

3.2. Thermal properties

The thermal stability of the polymers was characterized by thermogravimetric analysis (TGA). As shown in Fig. 1 and Table 1, the polymers, PC1–5 are thermally stable, with 5% weight-loss temperatures of 326, 320, 318, 327, and 317 °C, respectively. The thermal stability of the copolymers satisfied the requirement for their applications to PSCs and other electronic devices.

3.3. Optical properties

The UV-vis absorption spectra of the copolymers in dilute chloroform solution and in thin films are shown in Fig. 2 and Table 2. In the solution of PC1–5, the weak absorption peak at short wavelength ($\lambda = 350$ – 425 nm) originates from the π – π^* transition of the benzodithiophene units, while the strong absorption peak at long wavelength ($\lambda = 450$ – 550 nm) is due to intra-molecular charge transfer (ICT) between the donor and the acceptor units. In the film state, the maximum absorption peaks (λ_{max}) of PC3–5 are red-shifted by about 33–42 nm compared with those in solution. It implies that PC3–5 in solution have random coil structures

Table 2
Photo and electrochemical properties of copolymers.

Polymers	Absorbance [nm]		$\lambda_{\text{cut-off}}$ [nm]	E_{ox}^{a} [V]	HOMO ^b [eV]	LUMO ^c [eV]	$\Delta E_{\text{g}}^{\text{opt,d}}$ [eV]
	Solution	Film					
PC1	500, 534	505, 545	596	0.92	−5.32	−3.24	2.08
PC2	503	516	600	1.01	−5.41	−3.34	2.07
PC3	478	511	589	1.02	−5.42	−3.31	2.11
PC4	473	515	596	1.03	−5.44	−3.36	2.08
PC5	476	509	585	1.10	−5.50	−3.38	2.12

^a The oxidation potential (E_{ox}) was determined by $E_{\text{ox}}^{\text{onset}}$.

^b HOMO = $-e(4.4\text{V} + E_{\text{ox}}^{\text{onset}})$.

^c LUMO = $E_{\text{g}}^{\text{opt}} + \text{HOMO}$.

^d $E_{\text{g}}^{\text{opt}} = 1240/\lambda_{\text{cut-off}}$.

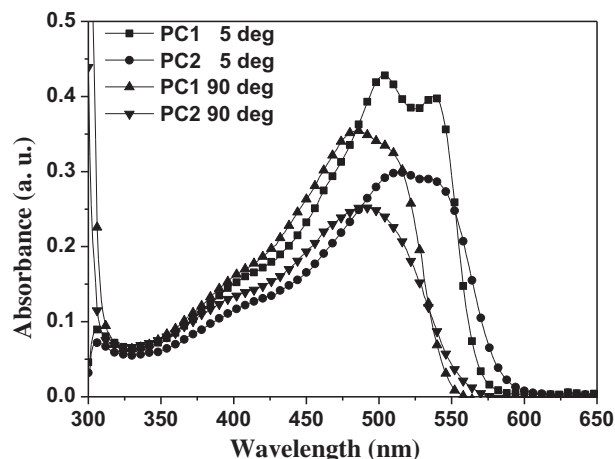


Fig. 3. UV-vis absorption spectra of PC1 and PC2 in the *o*-DCB solution at 5 °C and 90 °C.

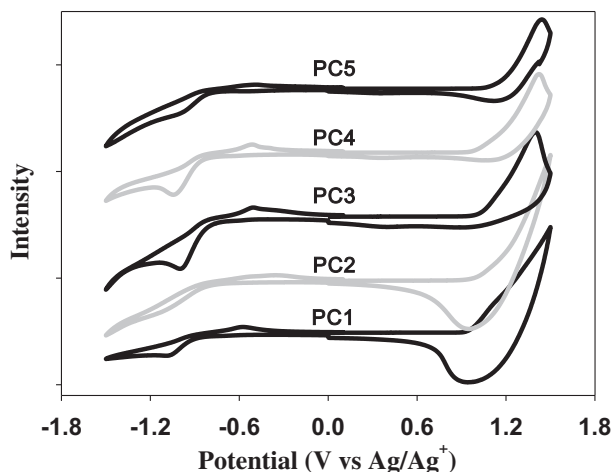


Fig. 4. Cyclic voltammogram of copolymer films on the platinum plate electrode in the acetonitrile solution containing 0.1 M Bu₄NPF₆ at a scan rate of 50 mV/s.

Table 3
OFET device performance of copolymers.

Polymers	W/L ratio	I_{on}/I_{off}	V_{th}	μ_{FET} (cm ² V ⁻¹ s ⁻¹)
PC1	15	104	-4	1.00×10^{-3}
PC2	15	103	-2	4.18×10^{-5}
PC3	15	103	-9	2.68×10^{-5}
PC4	15	104	-9	8.45×10^{-5}
PC5	15	102	-23	3.35×10^{-5}

and have the limited conjugation in the polymer main-chain because of the steric hindrance of relatively longer alkyl side-chain in polymer backbone. However, steric hindrance in the polymer films (PC3–5) is suppressed by intermolecular interactions between polymer backbones upon aggregation. In contrast, λ_{max} s of PC1 and PC2 in the film states showed a smaller red-shift ($\Delta\lambda = 11$ –13 nm), as compared to those in solution (Fig. 2). Interestingly, PC1 and PC2 showed strong thermochromic behaviors in the *o*-DCB solution (Fig. 3). At temperature over 90 °C, PC1 and PC2 showed a blue-shifted absorption band at λ_{max} s of 482 and 488 nm, respectively. However, by decreasing the temperature, the absorption spectra of PC1 and PC2 were significantly red-shifted and the spectral shapes at a low temperature are considerably similar to those of the film state. Also, the absorption range and the

spectral shape at high temperature are similar to those of the PC3–5 bearing relatively long and bulky alkyl side-chain groups. Therefore, the resulting absorption behaviors indicate that PC1 and PC2 have a very strong inter- and intra-chain interaction between the polymer chains even in the solution state [29]. These results mean that the methyl carboxylate group in PC2 did not hinder geometrical interactions and its optical behavior of PC2 in solution and in solid film states is similar to that of PC1 having a relatively planar backbone structure.

3.4. Electrochemical properties

Electrochemical analysis was performed to determine the redox ionization potentials of the synthesized copolymers. The highest occupied and lowest unoccupied molecular orbital (HOMO/LUMO) energy levels can be calculated from the electrochemical potentials, together with the absorption spectra. The cyclic voltammograms (CV) were recorded in a solution sample, and the potentials were obtained relative to an internal ferrocene reference (Fc/Fc⁺). E_{ox} of copolymers was obtained from the onset potentials of oxidation waves versus SCE. Fig. 4 presents the cyclic voltammograms of the copolymer films coated on the Pt plates. All polymers exhibit one quasi-reversible oxidation and one irreversible reduction processes; therefore, we were unable to estimate their LUMO energies accurately. In order to determine the LUMO levels, we combined the oxidation potential in CV with the optical bandgap energy (E_g^{opt}) resulting from the absorption edge in their absorption spectra. Comparing to the HOMO energy value of PC1 (–5.32 eV), the PC2–5 containing carboxylate unit showed deeper HOMO values of –5.41, –5.42, –5.44, and –5.50 eV, respectively. These results show that the alkyl carboxylate groups in copolymer PC2–5 are favorable to make a lower lying HOMO energy value compared to that of PC1. We also found that the HOMO value of TC-based copolymers was slightly increased by increasing the number of alkyl length into TC unit.

3.5. OTFT properties

The charge transport properties of copolymers were investigated by solution processed field-effect transistors (FETs). Thin films of the copolymers on *n*-octyltrichlorosilane (OTS)-treated SiO₂/Si wafers were deposited by spin-casting a solution of copolymers in chloroform. All the devices displayed typical *p*-type channel TFT performance. Copolymer PC1 exhibited good device

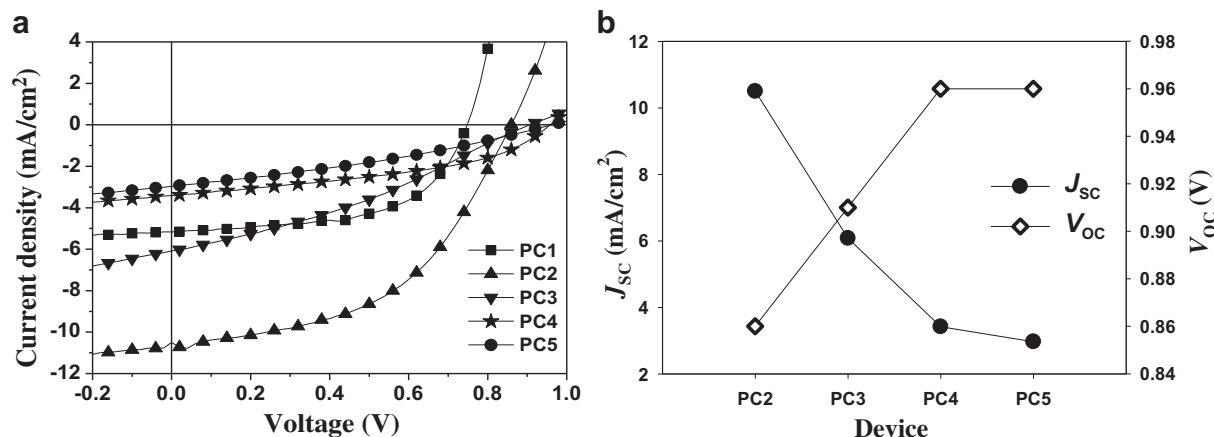


Fig. 5. Current density–voltage (J – V) characteristics of PV devices based on copolymer:PC₇₁BM (1:1 wt %) blends (a) and dependence of V_{oc} and J_{sc} of the different polymer:PCBM solar cells (b).

Table 4
Photovoltaic performances of copolymers under illumination of 100 mW/cm² white light.

Polymers	Polymer:PC ₇₁ BM [wt. %]	J_{sc} [mA/cm ²]	V_{oc} [V]	FF	PCE [%]
PC1	1:1	5.16	0.75	0.57	2.20
PC2	1:1	10.50	0.86	0.50	4.52 [27]
PC3	1:1	6.08	0.91	0.33	1.80
PC4	1:1	3.42	0.96	0.43	1.40
PC5	1:1	2.97	0.96	0.32	0.92

performance, with mobility up to $1.0 \times 10^{-3} \text{ cm}^2 \text{ V}^{-1} \text{ s}^{-1}$, and the hole mobility for PC2–5 are evaluated to be 4.18×10^{-5} , 2.68×10^{-5} , 8.45×10^{-5} , and $3.35 \times 10^{-5} \text{ cm}^2 \text{ V}^{-1} \text{ s}^{-1}$, respectively (Table 3). These results indicate that the alkyl chain of TC unit might interrupt the crystallinity of polymer film, resulting in reducing the hole mobility of PC2–5.

3.6. Photovoltaic properties

The photovoltaic properties of copolymers were studied in BHJ PSCs using PC₇₁BM as an acceptor in a conventional device configuration of ITO (indium tin oxide)/poly(3,4-ethylene dioxythiophene):poly(styrene sulfonate)(PEDOT:PSS)/polymer:PC₇₁BM (1:1 wt. ratio)/LiF/Al. In this study, the total concentration of polymer:PC₇₁BM(1:1 wt%) blend solution used for spin-coating active layer was 20 mg/mL, and *o*-dichlorobenzene was used as the solvent. All devices were post-annealed in a N₂ atmosphere for 10 min at 90 °C, before the deposition of the electrode. Fig. 5a

shows the current density–voltage (*J*–*V*) characteristics of the fabricated PV cells under simulated AM 1.5G solar illumination at 100 mW/cm². The results of the device performance are summarized in Table 4. Among the PV devices with PC1–5, the device composed of PC2:PC₇₁BM (1:1) showed the highest PCE of 4.52%. Compared to the PC1:PC₇₁BM (1:1) device ($V_{oc} = 0.75 \text{ V}$ and $J_{sc} = 5.16 \text{ mA/cm}^2$), the PC2-based device exhibited a better OPV performance, yielding a V_{oc} of 0.86 V and J_{sc} of 10.5 mA/cm² [27]. For a better understanding of the origin of the PV performance, electrochemical analysis and atomic force microscopy (AFM) were performed. The high V_{oc} value of the PC2-based PV device corresponds to the lower-lying HOMO level (–5.43 eV), compared to PC1 of –5.32 eV. As shown in Fig. 6a, the AFM surface image of the as-cast PC1:PC₇₁BM (1:1) blend film showed larger crystalline domain size compared to the PC2:PC₇₁BM (1:1) blend film [27]. It is likely that the PC2 polymer introducing methyl carboxylate could have much better compatibility with PC₇₁BM. Although the carrier mobility ($\mu = 1 \times 10^{-3} \text{ cm}^2 \text{ V}^{-1} \text{ s}^{-1}$) of PC1 is much higher than the other copolymers, the coarse domain of the film surface could decrease the interfacial area for exciton dissociation and effective percolation for charge transport in the blend film, thus lowering the J_{sc} of the PC1:PC₇₁BM device. Also, compared to the PC2-based device, the devices with PC3–5 showed higher V_{oc} values of 0.91, 0.96, and 0.96 V, respectively. These V_{oc} results are in good agreement with the measured HOMO values of copolymers in the cyclic voltammogram (CV) studies. However, by increasing the alkyl chain length in the TC unit, J_{sc} s of PC3–5 devices largely decreased as can be seen in Fig. 5b. It can be also supported by the difference in the AFM surface images of polymer:PC₇₁BM blend films. As

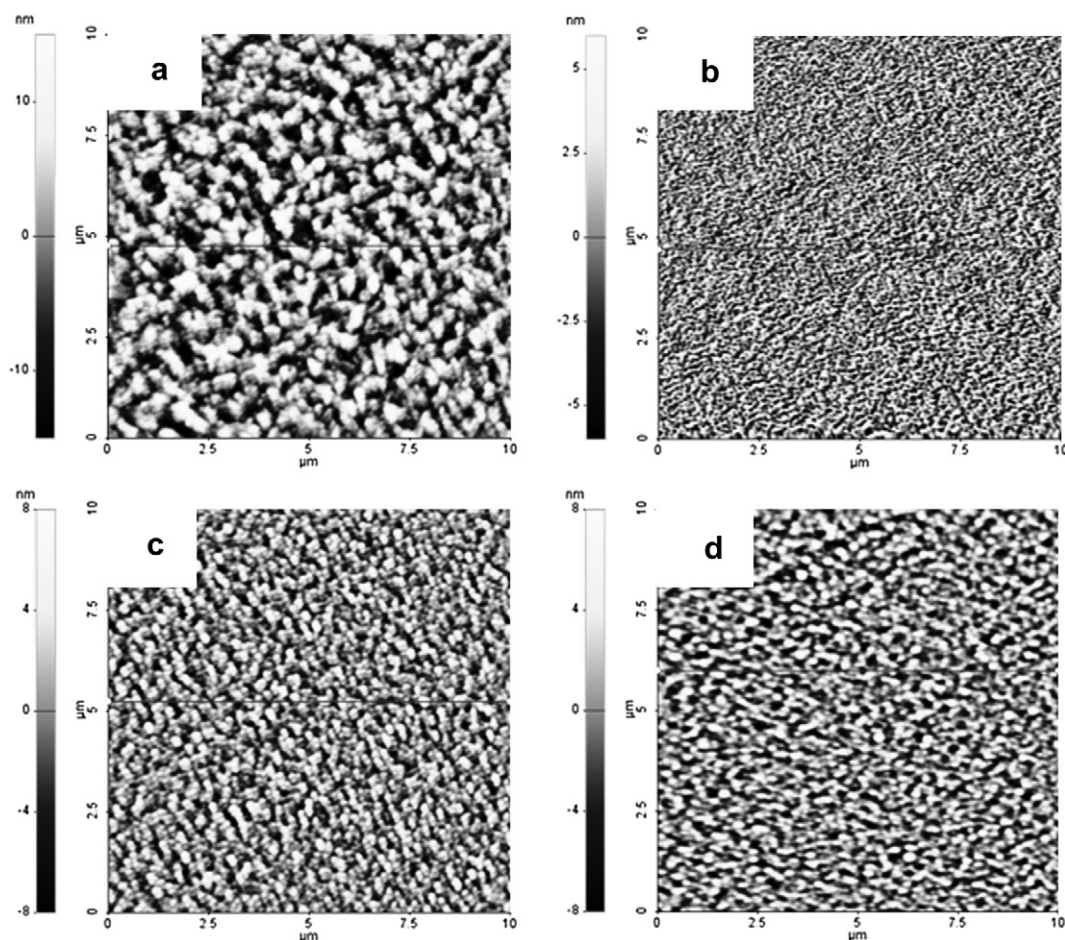


Fig. 6. AFM topographic view (10 × 10 μm) of the spin cast active layer; (a) PC1:PC₇₁BM(1:1), (b) PC3:PC₇₁BM(1:1), (c) PC4:PC₇₁BM(1:1), and (d) PC5:PC₇₁BM(1:1).

shown in Fig. 6, these films showed different domain size and the root mean square (RMS) roughness values of PC2–5 are 1.0 nm [27], 6.5 nm, 8.7 nm and 9.7 nm, respectively. The formation of larger domains and poor nanophase segregation can decrease the J_{SC} value due to a decrease in the interfacial area for the exciton dissociation between the polymer and PC₇₁BM. Herein, it could be understood that the photovoltaic properties of the TC-based copolymers are much dependent on alkyl chain length and bulkiness of the TC monomer unit.

4. Conclusions

To investigate the influence of the alkyl side-chain in TC-based copolymers on the device performance of BHJ PSCs, a soluble monomer of 4,8-bis(2-ethylhexyloxy)benzo[1,2-*b*:4,5-*b'*]dithiophene was successfully copolymerized with electron-rich alkyl substituted TC units with different alkyl chain length. The copolymers were designed to contain methyl, 1-butyl, 1-octyl, and 2-ethylhexyl thiophene-3-carboxylate units to yield the copolymers, PC2–5. These TC-based copolymers provide fairly low band gaps ($E_g = 2.0$ – 2.1 eV) with deeper HOMO energy levels (~ -5.4 eV) for obtaining a high V_{OC} value in BHJ PSCs, compared to PC1 without a TC unit. Among the OPV devices fabricated in this study, the PC2 as a donor and PC₇₁BM as an acceptor exhibited an efficient device performance, with a J_{SC} of 10.5 mA/cm² and a PCE of 4.52%. Meanwhile, the PC5-based device shows the highest V_{OC} of 0.96 V but its J_{SC} is relatively low due to more coarse film morphology. Therefore, the PCE of the PSC fabricated from PC5 was lower than 1%, even though it has a good V_{OC} value. In this study, it is found that the new TC-based copolymers are more useful to optimize the alkyl side-chain length in the TC unit for obtaining a high efficient PCE of BHJ solar cell. Currently some copolymers bearing new strong donor monomers such as cyclopenta[2,1-*b*:3,4-*b'*]dithiophene and dithieno[3,2-*b*:2',3'-*d*]pyrrole and methyl-substituted TC-based monomer, are being synthesized and their PV cells are being fabricated with PC₇₁BM. Their device performances are expected to show improvement compared to the results we obtained in this work.

Acknowledgment

This work was financially supported by the Air Force Office of Scientific Research (Grant No. FA95500910361) and the National Science Foundation (Grant No. DMR0702372). Partial support was also provided by the National Research Foundation of Korea Grant funded by the Korean Government (NRF-2009-352-D00080). DH Choi

particularly thank for the support by the NRF funded by the Ministry of Education, Science and Technology (NRF2012R1A2A1A01008797 and 20120005860).

References

- [1] Krebs FC. *Sol Energy Mater Sol Cells* 2009;93:394–412.
- [2] Krebs FC, Fyenbob J, Jørgensen M. *J Mater Chem* 2010;20:8994–9001.
- [3] Brabec CJ, Gowrisanker S, Halls JMM, Laird D, Jia S, Williams SP. *Adv Mater* 2010;22:3839–56.
- [4] Andersen TR, Larsen-Olsen TT, Andreasen B, Böttiger APL, Carlé JE, Helgesen M, et al. *ACS Nano* 2011;5:4188–96.
- [5] Bundgaard E, Hagemann O, Manceau M, Jørgensen M, Krebs FC. *Macromolecules* 2010;43:8115–20.
- [6] Sun Y, Seo JH, Takacs CJ, Seifter J, Heeger AJ. *Adv Mater* 2011;23:1679–83.
- [7] Bronstein H, Chen Z, Ashraf RS, Zhang W, Du J, Durrant JR, et al. *J Am Chem Soc* 2011;133:3272–5.
- [8] He F, Wang W, Chen W, Xu T, Darling SB, Strzalka J, et al. *J Am Chem Soc* 2011;133:3284–7.
- [9] Price SC, Stuart AC, Yang L, Zhou H, You W. *J Am Chem Soc* 2011;133:4625–31.
- [10] Small CE, Chen S, Subbiah J, Amb CM, Tsang SW, Lai TH, et al. *Nat Photonics* 2012;6:115–20.
- [11] Lee JK, Ma WL, Brabec CJ, Yuen J, Moon JS, Kim JY, et al. *J Am Chem Soc* 2008;130:3619–23.
- [12] Hou J, Chen HY, Zhang S, Chen RI, Yang Y, Wu Y, et al. *J Am Chem Soc* 2009;131:15586–7.
- [13] Liang YY, Wu Y, Feng DQ, Tsai ST, Son HJ, Li G, et al. *J Am Chem Soc* 2009;131:56–7.
- [14] Mühlbacher D, Scharber M, Morana M, Zhu Z, Waller D, Gaudiana R, et al. *Adv Mater* 2006;18:2884–9.
- [15] Peet J, Kim JY, Coates NE, Ma WL, Moses D, Heeger AJ, et al. *Nat Mater* 2007;6:497–500.
- [16] Hou J, Chen H, Zhang S, Li G, Yang Y. *J Am Chem Soc* 2008;130:16144–5.
- [17] Zhang F, Jespersen KG, Björström C, Svensson M, Andersson MR, Sundström V, et al. *Adv Funct Mater* 2006;16:667–74.
- [18] Wienk MM, Turbiez M, Gilot J, Janssen RAJ. *Adv Mater* 2008;20:2556–60.
- [19] Zou YP, Najari A, Berrouard P, Beaupré S, Aich BR, Tao Y, et al. *J Am Chem Soc* 2010;132:5330–1.
- [20] Brabec CJ, Cravino A, Meissner D, Sariciftici NS, Fromherz T, Rispen MT, et al. *Adv Funct Mater* 2001;11:374–80.
- [21] Piliago C, Holcombe TW, Douglas JD, Woo CH, Beaujuge PM, Fréchet JMJ. *J Am Chem Soc* 2010;132:7595–7.
- [22] Chu TY, Lu J, Beaupré S, Zhang Y, Pouliot JR, Wakim S, et al. *J Am Chem Soc* 2011;133:4250–3.
- [23] Amb CM, Chen S, Graham KR, Subbiah J, Small CE, So F, et al. *J Am Chem Soc* 2011;133:10062–5.
- [24] Su MS, Kuo CY, Yuan MC, Jeng US, Su CJ, Wei KH. *Adv Mater* 2011;23:3315–9.
- [25] Hu X, Shi M, Chen J, Zuo L, Fu L, Liu Y, et al. *Macromol Rapid Commun* 2011;32:506–11.
- [26] Nie Y, Zhao B, Tang P, Jiang P, Tian Z, Shen P, et al. *J Polym Sci Part A Polym Chem* 2011;49:3604–14.
- [27] Cho MJ, Seo J, Kim KH, Choi DH, Prasad PN. *Macromol Rapid Commun* 2012;33:146–51.
- [28] Huo L, Chen TL, Zhou Y, Hou J, Chen HY, Yang Y, et al. *Macromolecules* 2009;42:4377–80.
- [29] Murphy AR, Liu J, Luscombe C, Kavulak D, Fréchet JMJ, Kline RJ, et al. *Chem Mater* 2005;17:4892–9.